Article

Desferrioxamine B: Investigating the Efficacy of Hydrogels and Ethanol Gels for Removing Akaganeite and Maghemite from Dry Wooden Substrates

Stavroula Rapti [1], **Stamatis Boyatzis** [1], **Shayne Rivers** [2], **Athanasios Velios** [3] **and Anastasia Pournou** [1,*]

[1] Department of Conservation and Antiquities and Works of Art, University of West Attica, 12243 Athens, Greece
[2] West Dean College of Arts and Conservation, Chichester, West Sussex PO18 0QZ, UK
[3] Ligatus Research Centre, Chelsea College of Arts, University of the Arts London, London SW1P 4JU, UK
[*] Correspondence: pournoua@uniwa.gr

Abstract: Cultural heritage (CH) wooden artifacts are often stained by iron oxides/hydroxy-oxides, which may have detrimental effects on wood. Their removal is a common conservation practice, and it is usually achieved with non-eco-friendly chelators, such as ethylene diamine tetra acetic acid (EDTA) and diethylene triamine penta acetic acid (DTPA). Siderophores are green materials that have been recently explored as chelators, given the currently growing environmental concerns. This work investigated desferrioxamine B (DFO-B), a promising siderophore that has not been adequately studied for its potential in removing ferric oxides/hydroxy-oxides from dry CH wooden substrates. Mock-ups of maple (*Acer platanoides* L.) were artificially stained with akaganeite and maghemite, and DFO-B was employed via hydrogels (pH: 6.5 and 8.6) and ethanol gels. The chelator efficacy was assessed using Energy-Dispersive Spectroscopy (EDS), Attenuated Total Reflection–Fourier Transform Infrared Spectroscopy (ATR-FTIR), Scanning Electron Microscopy (SEM) and colorimetry. The hydrogels' impact on the wood was also assessed using ATR-FTIR and colorimetry. The obtained results demonstrate that the most effective DFO-B formulation was the alkaline hydrogel (pH 8.6), followed by the acidic (pH 6.5) hydrogel and the DFO-B ethanol gel. No differences in wood chemistry or color were recorded when using pH 6.5 or 8.6. The DFO-B ethanol gels were also proven to be potential alternatives to hydrogels for use with water-sensitive CH substrates.

Keywords: conservation; restoration; wood; chelators; desferrioxamine B; siderophores; agarose; cultural heritage; green chelators; ferric oxides; ferric hydroxy-oxides

1. Introduction

Wood is one of the most used materials in human history, and, thus, cultural heritage (CH) wooden artifacts provide important evidence of human culture and civilization [1,2] and constitute a legacy of sociocultural and economic value for all humanity [3]. Wooden artifact technology typically includes the use of metallic parts, such as handles, nails, knobs, keyhole frames and hinges, which corrode when found in environments with a relative humidity above 65%, forming iron oxides and/or hydroxy-oxides. Iron hydroxy-oxides usually include goethite (α-FeOOH), lepidocrocite (γ-FeOOH), akaganeite (β-FeOOH), feroxyhite (δ-FeOOH) and ferrihydrite ($Fe_5O_8 \bullet 4H_2O/5Fe_2O_3 \bullet 9H_2O$), whereas iron oxides include hematite (α-Fe$_2$O$_3$), maghemite (γ-Fe$_2$O$_3$) and magnetite (Fe$_3$O$_4$) [4–7]. These iron corrosion compounds may have detrimental effects on wooden substrates [6,8,9] and, therefore, their removal is a common practice, as it is essential for the long-term preservation and safeguarding of CH wooden artefacts.

In the field of CH conservation, the removal of these insoluble compounds from substrates, such as paintings, paper, textiles, metals, ceramics, stone and waterlogged wood, is commonly achieved with waterborne chelators, such as ethylene diamine tetra

acetic acid (EDTA) and diethylene triamine penta acetic acid (DTPA), which are capable of bonding with iron ions and of forming water-soluble complexes [10–16]. Nonetheless, studies on the application of these chelators to dry wooden substrates are scarce. In addition, chelators, such as EDTA and DTPA, do not comply with the current national legislations and international environmental restrictions that point toward safer and eco-friendlier materials, and, thus, their replacement has become critical [17].

Siderophores constitute a relatively new group of "green" chelators, with potential usage for removing harmful iron ions from cultural heritage substrates whilst minimizing environmental risks [18–23].

These green chelators are hexadentate ligands with a high affinity for ferric ion [23–25]. Furthermore, they inhibit Fenton reactions and, thus, prevent the production of damaging hydroxyl radicals, which is in contrast to conventional chelators, such as EDTA and DTPA [26].

Desferrioxamine B (DFO-B) is a siderophore that has been investigated in the conservation of paper [18,19] and waterlogged wood [21], where it is applied via immersion into its aqueous solutions so that stained substrates are fully impregnated. The only work on DFO-B application to dry substrates was undertaken by Rapti et al. (2017) [20], who examined DFO-B hydrogels in comparison to other chelators in order to explore its potential to remove iron oxides and/or hydroxy-oxides.

Hydrogels are regularly used for aqueous cleaning in the field of conservation, which is mostly due to their controlled moisture delivery [27,28]. Their main disadvantage is the remaining surface residues, which can be difficult to remove from porous or uneven substrates [28,29] and may alter substrate properties [30,31].

In the study conducted by Rapti et al. (2017) [20], however, the presence of hydrogel residues and their impact on wood were not chemically investigated. Furthermore, parameters such as application time and the effect of the clearance process by cotton swab were not considered.

Therefore, this work was set up to more thoroughly investigate the efficacy of desferrioxamine B in removing an iron hydroxy-oxide (akaganeite (β-FeOOH)) and an iron oxide (maghemite (γ-Fe$_2$O$_3$) frequently found on CH wooden objects. The commonly used conservation process of "clearance" with cotton swabs was avoided, as it may bias the DFO-B cleaning performance. The study employed pH-buffered DFO-B via agarose semi-rigid hydrogels in order to minimize the diffusion of the aqueous solutions into the hygroscopic wood without reducing the green chelator efficacy [32,33] and, at the same time, to lessen the possibility of surface residues.

Lastly, for CH wooden substrates that cannot tolerate aqueous cleaning, this study also examined the complexing potential of DFO-B when applied via ethanol gels.

2. Materials and Methods

2.1. Mock-Up Preparation

Wooden mock-ups were made of maple (*Acer platanoides* L.), as this European wood species is often used in wooden artifact manufacturing. Furthermore, the light color of the maple would allow for a better monitoring of the cleaning process, whereas its low content of tannins would not interfere with the artificial staining protocol. Samples with a 30 mm length and 22 × 5 mm cross-section (tangential × radial) were artificially stained via ferrous chloride, which was coated on their tangential surfaces (the staining protocol is not presented herein). The presence of oxides/hydroxy-oxides on each mock-up was estimated on an oven-dry weight basis before and after staining to be ~20 mg (average of 10 replicates). Mössbauer and ATR-FTIR spectroscopy showed that they consisted mostly of the ferric compounds akaganeite (β-FeOOH) and maghemite (γ-Fe$_2$O$_3$), whereas low quantities of ferrous compounds were also recorded with Mössbauer spectroscopy.

2.2. Cleaning Methodology

Desferrioxamine B mesylate salt (DFO-B) (Desferal® Novartis) was dissolved in deionized water (6×10^{-2} M). DFO-B is a hexadentate ligand, and it binds iron ions in a 1:1 stoichiometry (DFO-B:iron ion) to form stable complexes [24]; nonetheless, it was decided to adopt a lower stoichiometry of 0.5:1 in this study in order to achieve a more controlled and monitored cleaning process. Furthermore, this stoichiometry allowed for a better formation of rigid gels, which would be otherwise inhibited, as an increased concentration, along with the corresponding buffers, would produce high-ionic-strength solutions hardly possible to be gelled. The concentration of the DFO-B aqueous solution was calculated based on the iron oxide type and the average quantity of iron compounds present on each mock-up (~20 mg).

The pH of the solution was buffered at pH 6.5 with 0.1 M succinic acid (puriss pa. $\geq$ 99.5%, Sigma Aldrich, St. Louis, MO, USA) and 0.2 M of trizma base (puriss pa. $\geq$ 99.9%, Sigma Aldrich) and to 8.6 with 0.1 M boric acid (puriss pa. $\geq$ 99.8%, Honeywell) and 0.3 M trizma base in order to be compatible with the wooden substrate and, at the same time, to comply with the required dissociation constants (pK_a) of the chelator's complexing ability. The solution was gelled with 4% w/v agarose A0169 (Type I-A, Low EEO, Sigma Aldrich) at 85 °C. The DFO-B agarose gel (2 mL) was applied to the mock-up's tangential surface (22×30 mm) with a plastic spatula in a semi-rigid state at approximately 45 °C before reaching its gelling point (according to Sigma Aldrich, the gelling point of Agarose A0169 at 1.5% w/v is 37.5 °C). The semi-rigid state was selected, as it enables application to 3D CH artifacts. The DFO-B hydrogels were applied for 1 h on four mock-ups, which were covered with a polyethylene film to avoid water evaporation. Eight repeated applications were performed on each mock-up. The same process was also applied to four unstained mock-ups, used as controls, in order to assess the possible chemical impact of the DBO-B gels' pH on the wooden substrate. After every application of the hydrogels (pH: 6.5 and 8.6), a plain agarose rigid gel prepared in deionized water was placed two times on the cleaned surface for 15 min for clearance purposes [31,34].

For the ethanol gel, pure desferrioxamine mesylate salt (puriss pa. $\geq$ 92.5%, Sigma Aldrich) was also prepared at a concentration of 6×10^{-2} M in absolute ethanol (EtOH). DFO-B purchased from Sigma Aldrich was used instead of the Desferal® purchased from Novartis, since some excipients of the latter were insoluble in ethanol. The DFO-B/ethanol solution was applied via a 3 mm-thick rigid agarose gel (4% w/v in deionized water) that was cut in predefined dimensions (15×15 mm). Each gel piece was immersed for at least 12 h in a 2 mL DFO-B/ethanol solution. The gel was applied with plastic forceps on four mock-ups for 1 h, which were covered with a polyethylene film to avoid the evaporation of the solvent. In total, eight repetitions of this application were implemented on each mock-up. After the DFO-B/ethanol application, a plain agarose rigid gel prepared in deionized water was immersed for at least 12 h in ethanol, and it was placed on the cleaned surface twice.

2.3. Cleaning Efficacy

2.3.1. Scanning Electron Microscopy (SEM)

In order to observe the effectiveness of DFO-B in removing the formed iron corrosion products, the morphology of the substrates and any possible gel residues on the wooden mock-ups, Scanning Electron Microscopy (SEM) was performed before and after the 1st, 2nd, 4th and 8th application with a JEOL JSM–6510LV microscope at an accelerating voltage of 20 kV in a low-vacuum mode of 20–30 Pa.

Each mock-up was placed into the SEM vacuum chamber on a custom-made sample holder of Plexiglas®, which enabled the examination of the exact same area each time.

2.3.2. Energy-Dispersive X-ray Spectroscopy (EDS)

Energy-Dispersive X-ray Spectroscopy was performed on each wooden mock-up before, during and after the cleaning process with a JEOL JSM 6510 LV SEM, operated in a

low-vacuum mode of 20 Pa at an accelerating voltage of 20 kV, equipped with an Inca X–act silicon drift detector (SDD) with a PentaFET® Precision spectrometer (Oxford Instruments, Oxford, UK). Data were obtained and analyzed using Inca® software.

The iron (Fe) weight (%wt) was calculated with regard to the entire elemental profile of the organic substrate (C, O), excluding elements, such as Cl and Na, present due to staining or the cleaning procedure, respectively. The sample holder used for the SEM analysis was suitably adjusted so that the elemental analysis was performed on the exact same surface area of each mock-up before, during and after cleaning. The cleaning efficacy (%ΔFe) was calculated based on the difference between the weight of the iron detected before and after the cleaning using Equation (1):

$$\%\Delta\text{Fe} \ = \frac{\text{Fe}_{\text{before}} \ - \ \text{Fe}_{\text{after}}}{\text{Fe}_{\text{before}}} \times 100 \tag{1}$$

where:

$\text{Fe}_{\text{before}}$ = %wt of the detected Fe of a defined area before the DFO-B application;
Fe_{after} = %wt of the detected Fe of the same area after the DFO-B application.

2.3.3. Attenuated Total Reflection–Fourier Transform Infrared Spectroscopy (ATR-FTIR)

ATR-FTIR infrared spectra were recorded on the wooden mock-ups in order to investigate the removal of akageneite and maghemite and the possible presence of residues from the DFO-B agarose gels. ATR-FTIR was implemented using a BRUKER ALPHA II, in the ATR mode, equipped with a polycrystalline diamond crystal (RI 2.42), with a 2 mm-diameter active sample area. The mock-ups' tangential surfaces were placed on the ATR-FTIR crystal before and after the 8th cleaning application, and the spectra were recorded in the range of 4000 to 400 cm^{-1} (24 scans, resolution of 4 cm^{-1}). All recorded spectra were ATR-corrected using OPUS 8.5 SP1 software and accordingly baseline-corrected using SpectraGryph software v.1.2.16.1; no smoothing or other treatment of the spectra was carried out.

The thick layer of iron oxides/hydroxy-oxides on the mock-ups leveled down the characteristic infrared peaks and the shoulders of the wood. In order to better demonstrate the differences in the iron oxide/hydroxy-oxide quantities in a semi-quantitative manner, the spectra were further normalized using SpectraGryph software v.1.2.16.1, at 1032 cm^{-1} assigned to wood holocellulose C-O vibration, since it appears to be the least affected during the cleaning treatment (see the Section 3).

2.3.4. Colorimetry

To measure the color of the wooden substrates before and after each application, an X-Rite Lovibond portable spectrophotometer (SP60 RT series) was used, and the color difference (ΔE*) was calculated according to EN 15886:2010, using Equation (2). An average of three color measurements of the same area was recorded for the L*, a*, b* coordinates of the CIE LAB color space.

$$\Delta\text{E}^* \ = \sqrt{\Delta\text{L}^{*2} + \Delta\text{a}^{*2} + \Delta\text{b}^{*2}} \tag{2}$$

2.4. Cleaning Impact

The potential chemical alterations caused by the DFO-B hydrogels' pH (6.5 and 8.6) on the wood components were assessed on the four unstained controls using ATR-FTIR based on the methodology described in Section 2.3.3. Additionally, the peak ratio of lignin (1505 cm^{-1}) to carbohydrates (1736 cm^{-1}, 1370 cm^{-1}, 1237 cm^{-1} and 897 cm^{-1}) was calculated. These peaks' ratios were calculated using SpectraGryph software v.1.2.16.1 by measuring each peak area to its assigned suitable baseline limits. Furthermore, pure agarose powder A0169 (Type I-A, Low EEO, Sigma Aldrich) was also examined using ATR-FTIR as a reference to assist in the interpretation of any possible surface residues.
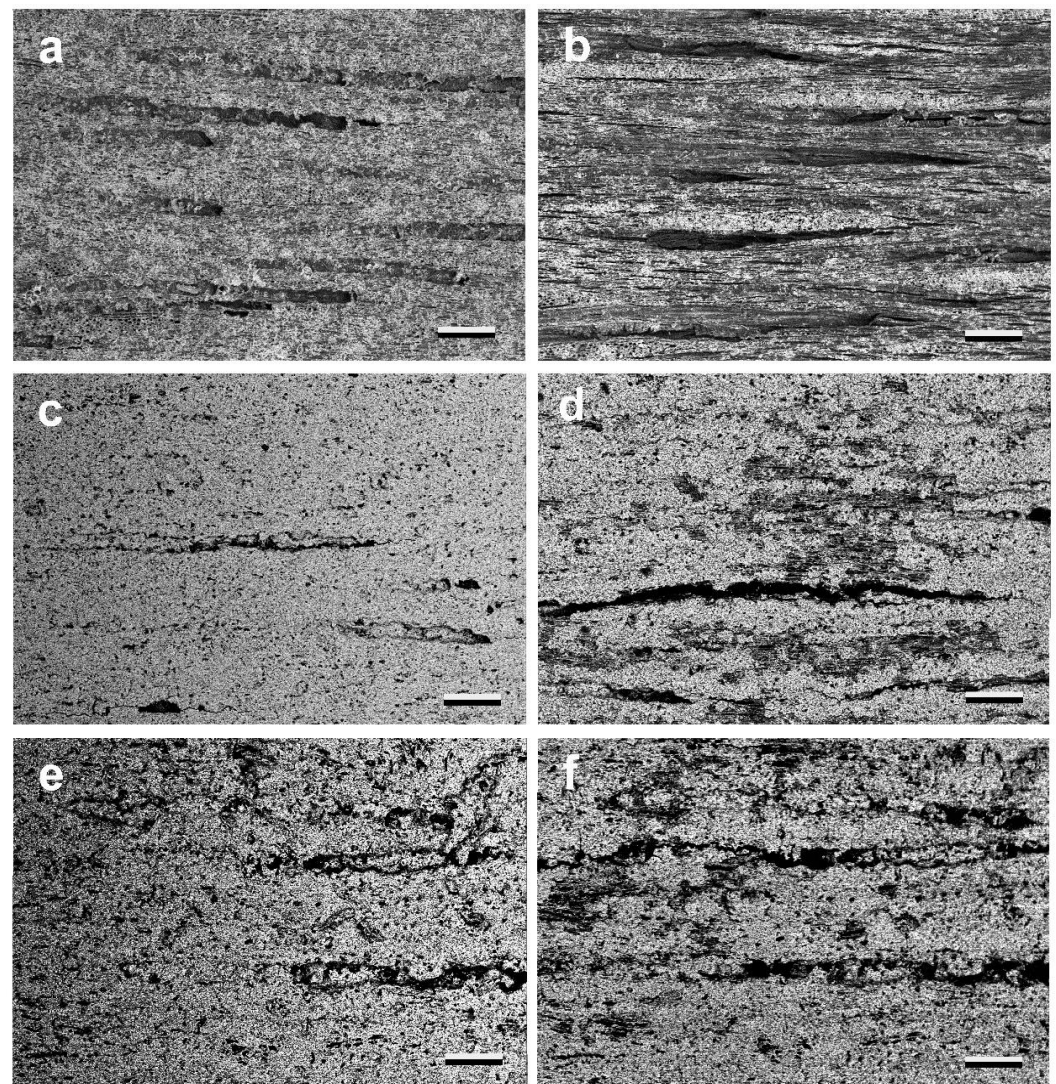
Wood color alterations due to the hydrogels' different pH values (6.5 and 8.6) were recorded on the four controls using colorimetry based on the methodology described in Section 2.3.4.
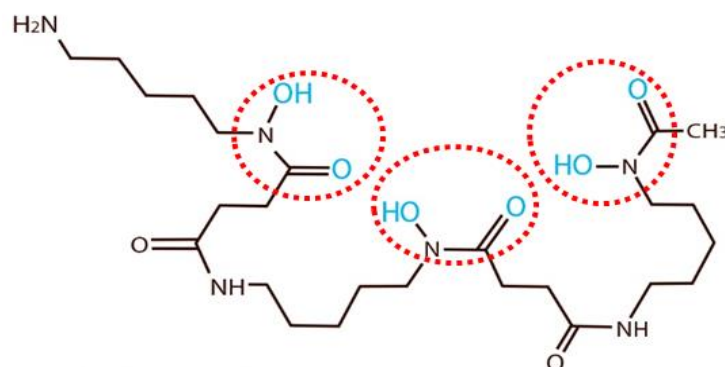
3. Results and Discussion

3.1. Cleaning Efficacy

3.1.1. Scanning Electron Microscopy (SEM)

The examination of the mock-ups with SEM, after the application of the DFO-B gels, showed that the formed iron compounds were removed at different depths depending on the DFO-B gel formulation applied (Figure 1). The most effective gel appeared to be the hydrogel of the DFO-B buffered at pH 8.6, since it was documented that wood cells covered with iron oxides became progressively visible with repeated gel applications (Figure 1b). This was rather anticipated, as pH 8.6 is close to the first pK_a of DFO-B (8.32) [35,36], and it indicates that the first ionized hydroxamate group was involved in the chelation process (Figure 2).

Figure 1. SEM micrographs of the stained mock-ups before the cleaning treatment (**a**,**c**,**e**) and of the same mock-ups after the 8th application of DFO-B at pH 8.6 (**b**), DFO-B at pH 6.5 (**d**) and DFO-B in EtOH (**f**), respectively. All scale bars = 100 μm.

Figure 2. Chemical structure of DFO-B with the functional groups that donate the electron pairs to a metal ion (highlighted in cyan) and the hydroxamate chemical groups that participate in the siderophore's molecule (circled in red).

The formation of iron–siderophore complexes is strongly pH-dependent [24,37,38], since it is related to the siderophore pK_{as} and its dissociation forms that promote complexation, and, thus, as anticipated, DFO-B was more effective when applied at alkaline pH.

However, alkaline pH values (over 9) have been reported to favor the alkaline hydrolysis of wood [39–41]. The examined alkaline DFO-B application, however, is considered harmless, as the contact time of the wood and the alkaline gel is relatively short compared to that of the impregnation treatments commonly used. Thus, the impact of this surface treatment was expected to be negligible.

Interestingly, the DFO-B buffered at 6.5 pH appeared also to be capable of removing the iron compounds (Figure 1d), even though, at this pH, the DFO-B was fully protonated (Table 1), and it was not expected to form complexes with the iron ions. According to Borer et al. (2009) [36], the DFO-B effectiveness in the pH range from 4 to 6 can be explained on the basis of an inner-sphere coordination of the undissociated –N–OH groups and the iron oxide/hydroxy-oxide surface. The acidic pH value of this regime is definitely more compatible with wooden substrates, and even if it presents inferior results compared to the alkaline DFO-B, it is considered that it can be equally effective with repeated applications. Furthermore, the SEM results demonstrated that the DFO-B in ethanol had the poorest cleaning performance (Figure 1f), as only a very thin layer of iron compounds appeared to be removed. Nonetheless, similarly to the acidic DFO-B, with repeated applications, this formulation can also be effective, and it can offer a useful alternative when waterborne solutions cannot be applied.
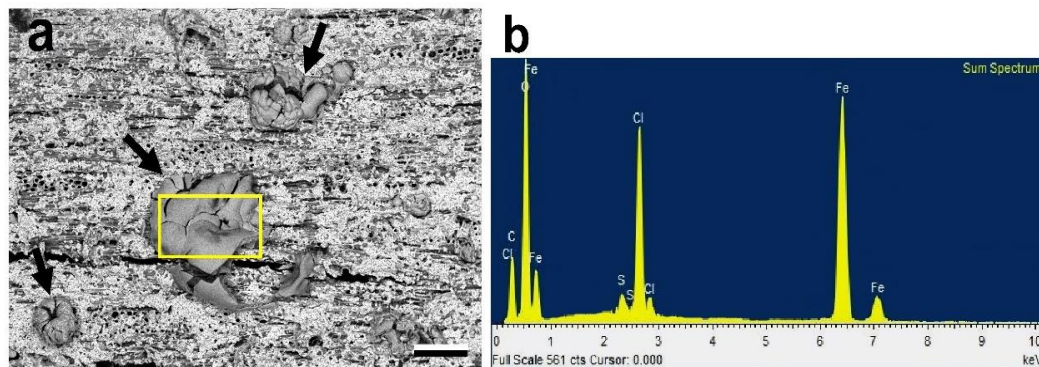
Table 1. Acid dissociation constant (pK_a) values of the hexadentate ligand DFO-B in accordance with the functional groups involved, adapted by ([a]) [35], ([b]) [25] and ([c]) [36].

Acid Dissociation Constant	Value (Functional Group)
pK_a1	8.32 [a]; 8.32 [b,c] (hydroxamate)
pK_a2	9.16 [a]; 8.96 [b,c] (hydroxamate)
pK_a3	9.94 [a]; 9.55 [b,c] (hydroxamate)
pK_a4	11.44 [a]; 10.79 [b] (hydroxamate)

The SEM analysis also documented that, during the 1st and 2nd applications of the alkaline DFO-B hydrogels, the formations of high iron, chlorine, carbon and oxygen contents were present on the surfaces of the mock-ups despite the clearance process (Figure 3). These formations, which were removed with repeated applications, were probably due to the large amount of formed iron/DFO-B complexes that were accumulated on the mock-ups' surfaces. A possible hypothesis is that this accumulation is related to the high affinity of the alkaline DFO-B for ferric ions, with this promoting the fast formation of iron complexes
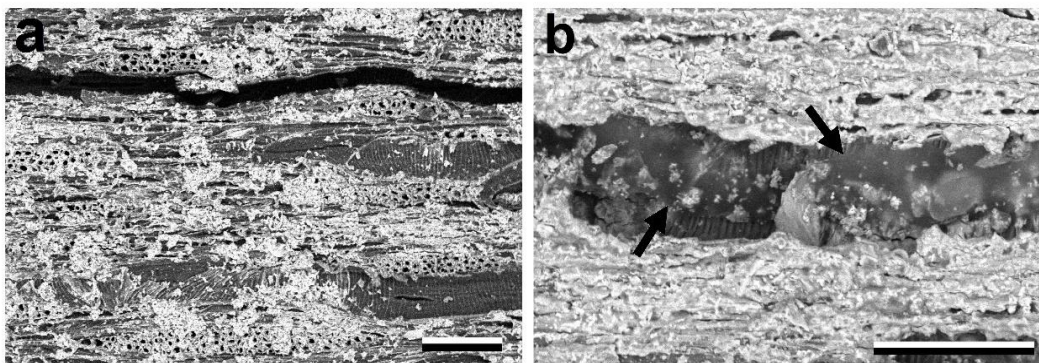
that were not removed from the surface when formed. Complexation visually occurred at ~15 min, when agarose became red due to the iron/DFO-B complex color [42]; however, based on the cleaning protocol, the hydrogel was removed after 1 h. Nonetheless, more research is considered necessary in order to comprehend the correlation of the gels' coloration during cleaning with the chelator's complexation capacity.

Figure 3. (**a**) SEM micrograph of a mock-up after the 1st application of the gelled DFO-B buffered at pH 8.6 showing formations (arrowed) that remained on the surface after cleaning, scale bar = 100 µm; (**b**) EDS elemental analysis of a formation.

　　The previous hypothesis agrees with the fact that the formations appeared only after the 1st and 2nd applications and suggests that they could be avoided if the application time was shorter or the clearance process was repeated and/or lasted longer. The same phenomenon was also observed, to a much lesser extent, however, with the acidic DFO-B hydrogels.

　　The examination with SEM also demonstrated that the use of the DFO-B agarose gels left no residues on the wooden mock-ups' tangential surfaces (Figure 4a). Extremely rarely, agarose residues only occurred on one mock-up, mainly in a vessels' lumen, when the DFO-B hydrogel was applied in the semi-rigid state (Figure 4b).
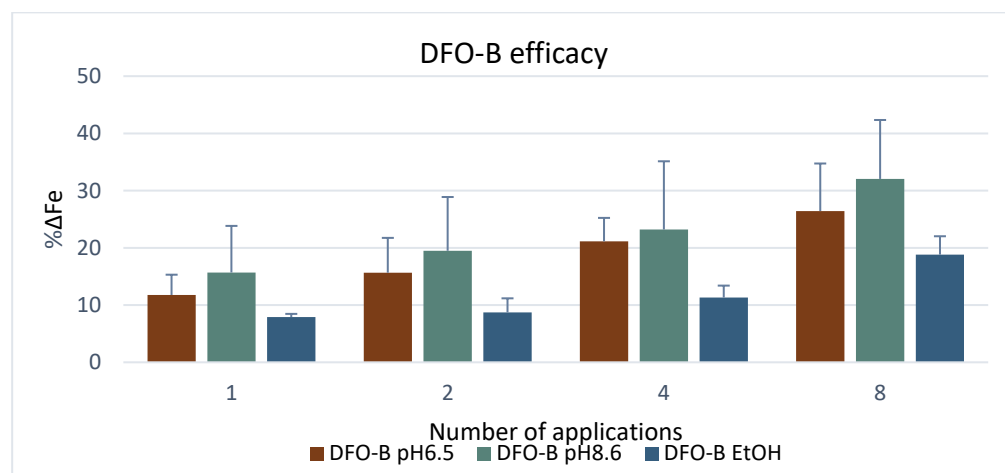

Figure 4. (**a**) SEM micrograph of a mock-up with no agarose residues; (**b**) SEM micrograph of mock-up where agarose residues (arrowed) are observed in a vessel lumen. Scale bars = 100 µm.

3.1.2. Energy-Dispersive X-ray Spectroscopy (EDS)

　　The EDS results are in agreement with those obtained from the SEM examination, and they confirm the efficacy of all three DFO-B formulations in removing the iron compounds from the dry wooden mock-ups. The %ΔFe was found to progressively increase with repeated applications, as expected. This trend of DFO-B efficacy, however, varied between the three formulations. More specifically, similar to the SEM results, after the 8th application, the alkaline hydrogel of the DFO-B presented higher %ΔFe values compared to the acidic DFO-B hydrogel, whereas the gelled DFO-B in ethanol presented the lowest

efficacy (Figure 5). This is in accordance with previous studies that investigated ferric ion removal from paper [18]. It needs to be noted, however, that the standard deviation (STDEV) values were rather high for both the alkaline and acidic gels, indicating a large variation in %ΔFe among the mock-ups, which is possibly due to the dissimilar quantity of the iron compounds formed during the artificial staining. Hence, when the initial concentration of the oxides on a mock-up surface was high, the recorded efficacy was low. This is also probably related to the ability of the given concentration of DFO-B to complex with a definite quantity of iron ions.

Figure 5. Cleaning efficacy (%ΔFe) calculated from iron weight (%wt) detected via EDS on mock-ups after 8 applications of DFO-B at pH 6.5, at pH 8.6 and dissolved in ethanol. All values are averages of four replicates.
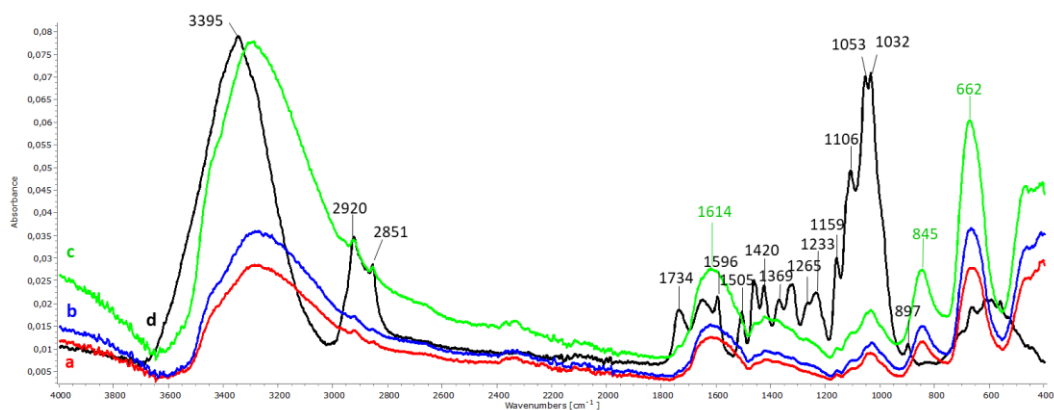
The variation in the alkaline DFO-B performance among the mock-ups could also be due to the diverse compositions of the iron oxides/hydroxy-oxides in the layers, consisting of both ferric and ferrous ions. The siderophore may have thus performed differently due to its higher stability constant for ferric ions ($logK_f$: 30.6) than for ferrous compounds ($logK_f$: 10) [24,43,44].

Nonetheless, even though these STDEV values are high, the DFO-B formulations still offer an efficient way for the removal of highly insoluble ferric oxides and hydroxy-oxides [5,23,24,45].

3.1.3. Attenuated Total Reflection–Fourier Transform Infrared Spectroscopy (ATR-FTIR)

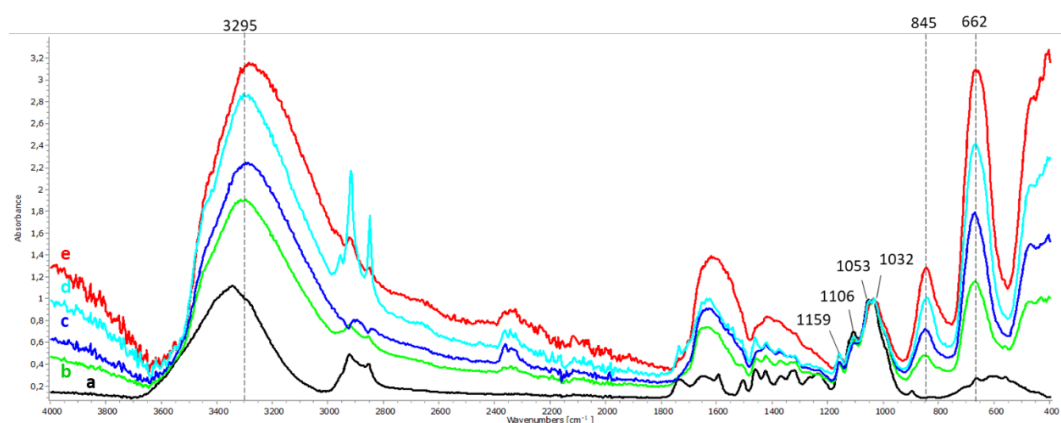The ATR-FTIR spectra of the maple reference sample (Figure 6d) clearly show the wood fingerprint peaks, including lignin at 1596 cm^{-1}, 1505 cm^{-1}, 1420 cm^{-1} and 1265 cm^{-1}; cellulose at 898 cm^{-1}; hemicellulose and pectins, both at 1734 cm^{-1} and 1233 cm^{-1} and holocellullose at 1369 cm^{-1}, 1153 cm^{-1} and 1032 cm^{-1} [46,47]. Nonetheless, the infrared bands of the stained wooden mock-ups before cleaning have a lower intensity and are featureless compared to those of the reference (Figure 6a–c) due to the masking of the wood by the layer of the iron oxides/hydroxy-oxides, of which the most dominant peaks are assigned to akageneite (845 cm^{-1} and 1614 cm^{-1}) and to maghemite (662 cm^{-1}).

Figure 6. ATR-FTIR spectra of three stained mock-ups before DFO-B application (**a**–**c**) in comparison to the maple reference spectrum (**d**). Spectra were ATR- and baseline-corrected, with no further treatment.

The spectra acquired after the cleaning well-reflected the different efficacies of the three DFO-B formulations applied to remove the iron oxides/hydroxy-oxides. This was mainly demonstrated by the gradual re-appearance of holocellulose features, such as the shoulders at 1159 cm^{-1}, 1106 cm^{-1}, 1053 cm^{-1} and 1032 cm^{-1}, after the 8th successive application of all DFO-B gels (hydrogels at pH 8.6, at pH 6.5 and ethanol gel) (Figure 7). Therefore, it was decided to normalize all spectra at the holocellulose peak of 1032 cm^{-1} in order to "monitor" the removal of the iron oxides/hydroxy-oxides from the wood. Furthermore, the DFO-B efficacy was able to be additionally demonstrated by the progressive decrease in the peaks at 845 cm^{-1} and 662 cm^{-1}, attributed to akaganeite and maghemite, respectively [5,48–50]. The ATR-FTIR analysis also showed that the siderophore efficacy was pH-dependent, confirming the SEM and the EDS results. Furthermore, it was also shown that the alkaline DFO-B hydrogels performed better (Figure 7b) than the acidic ones (Figure 7c), whereas the gel of the DFO-B in ethanol showed the poorest efficacy (Figure 7d).
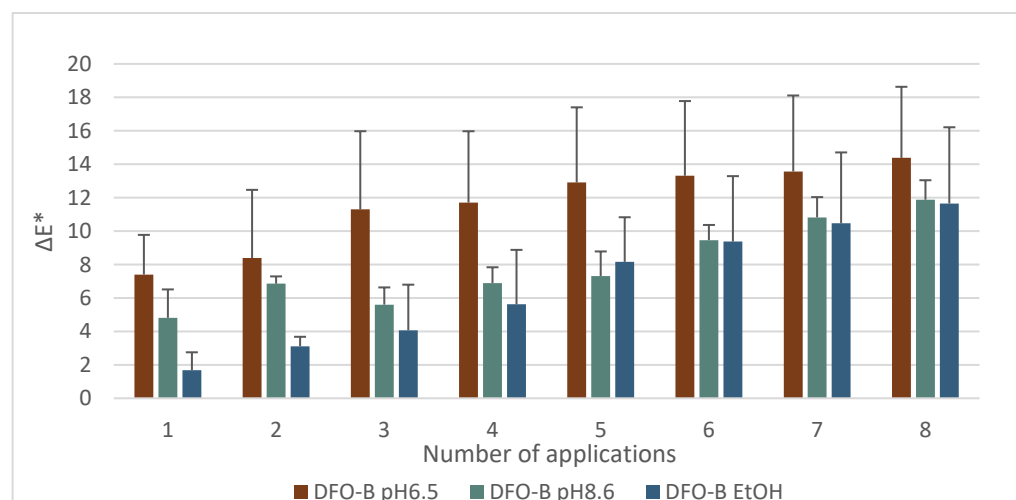

Figure 7. ATR-FTIR spectra of mock-ups after 8 applications of DFO-B at pH 8.6 (**b**), at pH 6.5 (**c**) and dissolved in ethanol (**d**) in comparison to the maple reference spectrum (**a**) and a stained mock-up before the cleaning treatment (**e**). Spectra were normalized with respect to the holocellulose peak at 1032 cm^{-1}.

3.1.4. Colorimetry

The calculated ΔE* represents the difference in color due to the DFO-B application, and, thus, the higher the ΔE*, the better the cleaning efficacy of the siderophore. The ΔE* values were shown to progressively increase with repeated applications (Figure 8). The highest ΔE* values were recorded on the 8th application with the acidic DFO-B hydrogel, whereas the ethanol gel showed slightly lower ΔE* values compared to the alkaline hydrogel (Figure 8).

These results though are not in accordance with those obtained from SEM, EDS and ATR-FTIR, which demonstrated that the alkaline DFO-B hydrogel performed best. A hypothesis for this disaccord could be the high efficacy of the alkaline DFO-B hydrogel to complex and rapidly solubilize the iron oxides/hydroxy-oxides, which, in turn, allowed for the diffusion of some diluted iron complexes into the wood. This may be avoided by reducing the application time and/or by increasing the duration/repetition of the clearance process.
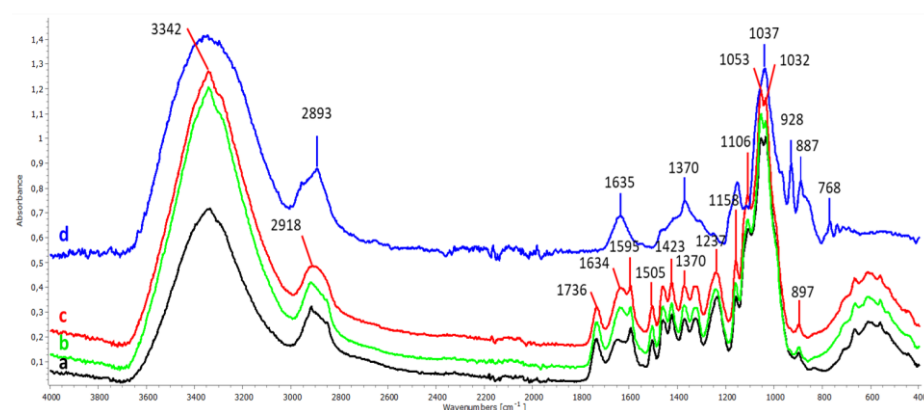

Figure 8. ΔE* of mock-ups after the 8th application of DFO-B hydrogels at pH 6.5 and pH 8.6 and the ethanol gel (EtOH). All ΔE* values are averages of four replicates.

3.2. Assessment of Hydrogels' Impact

3.2.1. ATR-FTIR

The ATR-FTIR spectra of the unstained controls recorded before and after the application of the DFO-B hydrogels at pH 6.5 and at pH 8.6 showed very small changes in the characteristic wood infrared bands, which are within experimental error (Figure 9). In both DFO-B applications, the increased maxima at $1637~cm^{-1}$ and $3342~cm^{-1}$, assigned to hydroxyls, are probably due to the water absorbed during the applications.

Figure 9. ATR-FTIR spectra of the control mock-ups after the 8th application of DFO-B at pH 8.6 (**b**) and pH 6.5 (**c**) in comparison to the spectrum acquired before application (**a**) and to a pure agarose spectrum (**d**).

The infrared band area ratios of the selected carbohydrate peaks against the lignin peak at $1505~cm^{-1}$, which is considered the least affected during the DFO-B applications, are shown in Table 2. More specifically, the $1505/1736~cm^{-1}$ ratio was slightly increased by 0.1, suggesting a minimal removal of hemicelluloses, while the $1505/897~cm^{-1}$ ratio was

also slightly increased by 0.24, indicating a decrease in the cellulose fraction; however, these increases are considered an insignificant impact of DFO-B on wood. Finally, negligible differences within experimental error were also marked for both 1505/1370 cm^{-1} and 1505/1237 cm^{-1} ratios. However, further research is considered necessary in order to establish the chemical interrelations between DFO-B formulations and wood components.
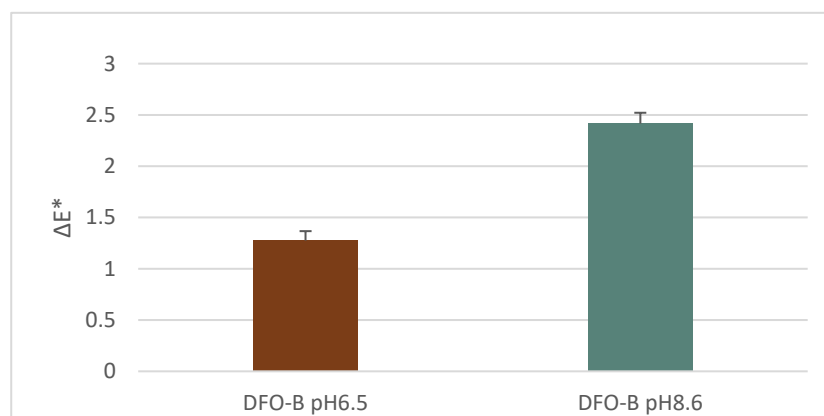
Table 2. Average ratios of the areas under the band maxima of aromatic lignin peak (1505 cm^{-1}) to typical carbohydrate peaks of wood (1736 cm^{-1}, 1370 cm^{-1}, 1237 cm^{-1} and 897 cm^{-1}) of four replicates before and after 8 DFO-B hydrogel applications.

Peak Ratios of Lignin to Carbohydrates:	1505/1736	1505/1370	1505/1237	1505/897
Controls before DFO-B	0.31 ($\pm$0.066)	1.03 ($\pm$0.154)	0.16 ($\pm$0.013)	1.82 ($\pm$0.250)
Controls after DFO-B at pH 6.5	0.41 ($\pm$0.037)	0.91 ($\pm$0.060)	0.18 ($\pm$0.009)	2.01 ($\pm$0.186)
Controls after DFO-B at pH 8.6	0.36 ($\pm$0.006)	0.87 ($\pm$0.005)	0.17 ($\pm$0.002)	2.06 ($\pm$0.0012)

Lastly, the spectra obtained from the controls after the application of the DFO-B hydrogels (Figure 9b,c) showed no agarose residues on the wood surface. This was clearly demonstrated when the spectra were compared to a pure agarose spectrum (Figure 9d), as the intensive agarose peaks at 1370 cm^{-1}, 1037 cm^{-1}, 928 cm^{-1}, 887 cm^{-1} and 768 cm^{-1} were absent.

3.2.2. Colorimetry

The colorimetry results regarding the ΔE* values obtained after the application of the DFO-B hydrogels at pH 6.5 and at pH 8.6 on the unstained controls are shown in Figure 10. The alkaline DFO-B presented a very small increase in ΔE* compared to the acidic one; however, this increase had a negligible impact on the color of the wood.

Figure 10. ΔE* of the controls after the 8th application of DFO-B hydrogels at pH 6.5 and 8.6. All ΔE* values are averages of four replicates.

4. Conclusions

This work demonstrated that DFO-B hydrogels and ethanol gels are capable of complexing the ferric ion of insoluble compounds, such as maghemite and akageneite, often encountered on CH wooden objects.

The results obtained from SEM, EDS and ATR-FTIR clearly demonstrated that DFO-B performed better in alkaline pH than in acidic or in ethanol formulations. The use of the alkaline hydrogel buffered at 8.6 pH was shown to not have an effect on the wood chemistry or color despite the wood's vulnerability to alkaline hydrolysis.

　　　　The DFO-B dissolved in ethanol had the poorest efficacy; however, with repeated applications, its effectiveness may increasingly be improved, making this gel formulation appropriate for use as a good alternative to hydrogels for water-sensitive CH substrates.

　　　　Furthermore, it was shown that the concentration, the time of application and the clearance steps may play important roles in the efficacy of this green siderophore, and, thus, further investigation is considered necessary in order to determine the most suitable parameters for the maximal removal of iron oxides/hydroxy-oxides.

　　　　Lastly, the detection of agarose residues was extremely rare, demonstrating that the adopted cleaning methodology can overcome this drawback of gels.

References

1. Nilsson, T.; Rowell, R. Historical Wood—Structure and Properties. In Proceedings of the International Conference, COST Action IE0601, Wood Science for Conservation of Cultural Heritage, Florence, Italy, 8–10 November 2007; Uzielli, L., Ed.; University Press: Firenze, Italy, 2009; pp. 11–15.
2. Monaco, A.; Balletti, F.; Pelosi, C. Wood in Cultural Heritage Properties and Conservation of Historical Wooden Artefacts. *Eur. J. Sci. Theol.* **2018**, *14*, 161–171.
3. Pournou, A. Preface. In *Biodeterioration of Wooden Cultural Heritage*; Organisms and Decay Mechanisms in Aquatic and Terrestrial Ecosystems; Springer Nature: Cham, Switzerland, 2020; pp. vii–viii. ISBN 978-3-030-46503-2.
4. Zhao, J.; Huggrns, F.E.; Feng, Z.; Huffman, G.P. Ferrihydrite: Surface Structure and Its Effects on Phase Transformation. *Clays Clay Min.* **1994**, *42*, 737–746. [CrossRef]
5. Cornell, R.M.; Schwertmann, U. *The Iron Oxides: Structure, Properties, Reactions, Occurrences, and Uses*, 2nd ed.; Wiley-VCH: Heppenheim, Germany, 2003; pp. 1–363. ISBN 3527302743.
6. Scott, D.A.; Eggert, G. *Iron and Steel in Art: Corrosion, Colorants, Conservation*; Archetype Publications: London, UK, 2009; pp. 35–105. ISBN 9781904982050.
7. Dai, N.; Zhang, J.; Chen, Q.; Yi, B.; Cao, F.; Zhang, J. Effect of the Direct Current Electric Field on the Initial Corrosion of Steel in Simulated Industrial Atmospheric Environment. *Corros. Sci.* **2015**, *99*, 295–303. [CrossRef]
8. Baker, A.J. Corrosion of Metal in Wood Products. In *Durability of Building Materials and Components. ASTM STP 691*; Sereda, P.J., Litvan, G.G., Eds.; American Society for Testing and Materials: West Conshohocken, PA, USA, 1980; pp. 981–993. ISBN 978-0-8031-4768-3.
9. Emery, J.A.; Schroeder, H.A. Iron-Catalyzed Oxidation of Wood Carbohydrates. *Wood Sci. Technol.* **1974**, *8*, 123–137. [CrossRef]
10. Burgess, H. The Use of Chelating Agents in Conservation Treatments. *Pap. Conserv.* **1991**, *15*, 36–44. [CrossRef]
11. Phenix, A.; Burnstock, A. The Removal of Surface Dirt on Paintings with Chelating Agents. *Conservator* **1992**, *16*, 28–38. [CrossRef]
12. Timár-Balázsy, Á.; Mátéfy, G.; Csányi, S. Effect of Stains and Stain Removal on Historical Textiles. In Proceedings of the 10th Triennial Meeting of ICOM Committee for Conservation, Washington, DC, USA, 22–27 August 1993; Bridgland, J., Ed.; ICOM–CC: Paris, France, 1993; pp. 330–335.
13. Rivers, S.; Umney, N. *Conservation of Furniture*; Butterworths-Heinemann: Oxford, UK, 2003; pp. 540–548. ISBN 0750609583.
14. Almkvist, G.; Dal, L.; Persson, I. Extraction of Iron Compounds from VASA Wood. In Proceedings of the 9th ICOM-CC Group on Wet Organic Archaeological Materials Conference, Copenhagen, Denmark, 7–11 June 2004; Hoffmann, P., Spriggs, J.A., Strætkvern, K., Gregory, D., Eds.; ICOM: Bremerhaven, Germany, 2005; pp. 202–210.
15. Macchia, A.; Ruffolo, S.A.; Rivaroli, L.; Russa, M.F. The Treatment of Iron-Stained Marble: Toward a "Green" Solution. *Int. J. Conserv. Sci.* **2016**, *7*, 323–332.
16. Thorn, A. Treatment of Heavily Iron-Stained Limestone and Marble Sculpture. In Proceedings of the 14th Triennial ICOM-CC Meeting, Hague, The Netherlands, 12–16 September 2005; Verger, I., Ed.; James and James/Earthscan: London, UK, 2005; pp. 888–894.

17. Balliana, E.; Ricci, G.; Pesce, C.; Zendri, E. Assessing the Value of Green Conservation for Cultural Heritage: Positive and Critical Aspects of Already Available Methodologies. *Int. J. Conserv. Sci.* **2016**, *7*, 185–202.
18. Wagner, B.; Bulska, E. Towards a New Conservation Method for Ancient Manuscripts by Inactivation of Iron via Complexation and Extraction. *Anal. Bioanal. Chem.* **2003**, *375*, 1148–1153. [CrossRef] [PubMed]
19. Bulska, E.; Wagner, B. Investigation of a Novel Conservation Procedure for Historical Documents. In *Cultural Heritage Conservation and Environmental Impact Assessment by Non-Destructive Testing and Micro-Analysis*; Grieken, R.V., Janssens, K., Eds.; Taylor & Francis-A.A Balkema: London, UK, 2005; pp. 101–116. ISBN 9058096815.
20. Rapti, S.; Boyatzis, S.; Rivers, S.; Velios, A.; Pournou, A. Removing Iron Stains from Wood and Textile Objects: Assessing Gelled Siderophores as Novel Green Chelators. In Proceedings of the Gels in Conservation Conference, London, UK, 16–18 October 2017; Angelova, L., Ormsby, B., Townsend, J., Wolbers, R., Eds.; Archetype Publications: London, UK, 2017; pp. 343–348, ISBN 9781909492509.
21. Albelda-Berenguer, M.; Monachon, M.; Joseph, E. Siderophores: From Natural Roles to Potential Applications. In *Advances in Applied Microbiology*; Gadd, G.M., Sariaslani, S., Eds.; Academic Press Inc.: London, UK, 2019; Volume 106, pp. 211–218. ISBN 9780128169759.
22. Monachon, M.; Albelda-Berenguer, M.; Joseph, E. Bio-based Treatment for the Extraction of Problematic Iron Sulphides from Waterlogged Archaeological Wood. In Proceedings of the 14th Wet Organic Archaeological Materials Conference, Portsmouth, UK, 20–24 May 2019; pp. 46–47.
23. Rapti, S.; Boyatzis, S.C.; Rivers, S.; Pournou, A. Siderophores and Their Applications in Wood, Textile, and Paper Conservation. In *Microorganisms in the Deterioration and Preservation of Cultural Heritage*; Joseph, E., Ed.; Springer: Cham, Switzerland, 2021; pp. 301–339. [CrossRef]
24. Hider, R.C.; Kong, X. Chemistry and Biology of Siderophores. *Nat. Prod. Rep.* **2010**, *27*, 637–657. [CrossRef]
25. Bellotti, D.; Remelli, M. Deferoxamine B: A Natural, Excellent and Versatile Metal Chelator. *Molecules* **2021**, *26*, 3255. [CrossRef] [PubMed]
26. Strlič, M.; Kolar, J.; Pihlar, B. Some Preventive Cellulose Antioxidants Studied by an Aromatic Hydroxylation Assay. *Polym. Degrad. Stab.* **2001**, *73*, 535–539. [CrossRef]
27. Khandekar, N. Gelled Systems: Theory and Early Application. In *Solvent Gels for the Cleaning of Works of Art: The Residue Question*; Dorge, V., Ed.; Getty Conservation Institute: Los Angeles, CA, USA, 2004; pp. 5–11. ISBN 0892367598.
28. Baglioni, P.; Chelazzi, D.; Giorgi, R. Innovative Nanomaterials: Principles, Availability and Scopes. In *Nanotechnologies in the Conservation of Cultural Heritage*; Springer: Dordrecht, The Netherlands, 2015; pp. 1–14. [CrossRef]
29. Stulik, D.; Wolbers, R. Project Outcome, Spin-Offs, and Future Research Needs. In *Solvent Gels for the Cleaning of Works of Art: The Residue Question*; Dorge, V., Ed.; Getty Conservation Institute: Los Angeles, CA, USA, 2004; pp. 131–152. ISBN 0892367598.
30. Larochette, Y. Determining the Efficacy of Cyclododecane as a Barrier for a Reduction Bleaching Treatment of a Silk Embroidered Linen Napkin. In Proceedings of the Textile Specialty Group Postprints of the 32nd AIC Annual Meeting, Portland, Oregon, USA, 9–14 June 2004; Randolph, J., MacKay, K., Hanson, R.M., Eds.; Textile Specialty Group of the American Institute for Conservation of Historic & Artistic Works (AIC): Washington DC, USA, 2004; Volume 14, pp. 1–10, ISSN 11524-3664.
31. Shaeffer, E.; Gardiner, J. New and Current Materials and Approaches for Localized Cleaning in Textile Conservation. In Proceedings of the Textile Specialty Group Postprints of the 41st AIC Annual Meeting, Indianapolis, IN, USA, 29 May–1 June 2013; Holden, A., Summerour, R., Schuetz, E., Carlson, J., Petersen, G., Eds.; Textile Specialty Group of the American Institute for Conservation of Historic & Artistic Works: Washington, DC, USA, 2013; Volume 23, pp. 109–124, ISSN 2169-1363.
32. Wolbers, R.; Sterman, N.; Stavroudis, C. *Notes for the Workshop on New Methods in the Cleaning of Paintings*; The Getty Conservation Institute: Los Angeles, CA, USA, 1990; pp. 5–45.
33. Wolbers, R. *Cleaning Painting Surfaces: Aqueous Methods*; Archetype: London, UK, 2000; pp. 81–125. ISBN 1873132360.
34. Cremonesi, P.; Casoli, A. Thermo-reversible Rigid Agar Hydrogels: Their Properties and Action in Cleaning. In *Preprints of Gels in Conservation Conference, London, UK, 16–18 October 2017*; Angelova, L., Ormsby, B., Townsend, J., Wolbers, R., Eds.; Archetype Publications: London, UK, 2017; pp. 19–28. ISBN 9781909492509.
35. Ihnat, P.M.; Robinson, D.H. Potentiometric Determination of the Thermodynamic Ionization Constants of Deferoxamine. *J. Pharm. Sci.* **1993**, *82*, 110–112. [CrossRef] [PubMed]
36. Borer, P.; Hug, S.J.; Sulzberger, B.; Kraemer, S.M.; Kretzschmar, R. ATR-FTIR Spectroscopic Study of the Adsorption of Des-ferrioxamine B and Aerobactin to the Surface of Lepidocrocite (γ-FeOOH). *Geochim. Cosmochim. Acta* **2009**, *73*, 4661–4672. [CrossRef]
37. Miethke, M.; Marahiel, M.A. Siderophore-Based Iron Acquisition and Pathogen Control. *Microbiol. Mol. Biol. Rev.* **2007**, *71*, 413–451. [CrossRef] [PubMed]
38. Ahmed, E.; Holmström, S.J.M. Siderophores in Environmental Research: Roles and Applications. *Microb. Biotechnol.* **2014**, *7*, 196–208. [CrossRef] [PubMed]
39. Unger, A.; Schniewind, A.P.; Unger, W. *Conservation of Wood Artifacts: A Handbook*; Springer: Berlin/Heidelberg, Germany, 2001; pp. 43–104. ISBN 3540415807.
40. Fors, Y.; Richards, V. The Effects of the Ammonia Neutralizing Treatment on Marine Archaeological Vasa Wood. *Stud. Conserv.* **2010**, *55*, 41–54. [CrossRef]

41. Pecoraro, E.; Pelé-Meziani, C.; Macchioni, N.; Lemoine, G.; Guilminot, E.; Pizzo, B. Effects of Iron Removal Treatments on the Chemical and Viscoelastic Properties of Waterlogged Wood. *J. Cult. Herit.* **2022**, *56*, 149–158. [CrossRef]
42. Domínguez-Vera, J.M. Iron(III) Complexation of Desferrioxamine B Encapsulated in Apoferritin. *J. Inorg. Biochem.* **2004**, *98*, 469–472. [CrossRef] [PubMed]
43. Raymond, K.N.; Müller, G.; Matzanke, B.F. Complexation of Iron by Siderophores a Review of Their Solution and Structural Chemistry and Biological Function. In *Structural Chemistry. Topics in Current Chemistry*; Boschke, F.L., Ed.; Springer: Berlin, Germany, 1984; Volume 123, pp. 49–102. [CrossRef]
44. Sharpe, P.C.; Richardson, D.R.; Kalinowski, D.S.; Bernhardt, P.V. Synthetic and Natural Products as Iron Chelators. *Curr. Top. Med. Chem.* **2011**, *11*, 591–607. [CrossRef]
45. Crumbliss, A.L. Iron Bioavailability and the Coordination Chemistry of Hydroxamic Acids. *Coord. Chem. Rev.* **1990**, *105*, 155–179. [CrossRef]
46. Chang, H.T.; Yeh, T.F.; Chang, S.T. Comparisons of Chemical Characteristic Variations for Photodegraded Softwood and Hardwood with/without Polyurethane Clear Coatings. *Polym. Degrad. Stab.* **2002**, *77*, 129–135. [CrossRef]
47. Pandey, K.K.; Pitman, A.J. Examination of the Lignin Content in a Softwood and a Hardwood Decayed by a Brown-Rot Fungus with the Acetyl Bromide Method and Fourier Transform Infrared Spectroscopy. *J. Polym. Sci. A Polym. Chem.* **2004**, *42*, 2340–2346. [CrossRef]
48. Rémazeilles, C.; Refait, P. On the Formation of β-FeOOH (Akaganéite) in Chloride-Containing Environments. *Corros. Sci.* **2007**, *49*, 844–857. [CrossRef]
49. Stoia, M.; Istratie, R.; Păcurariu, C. Investigation of Magnetite Nanoparticles Stability in Air by Thermal Analysis and FTIR Spectroscopy. *J. Therm. Anal. Calorim.* **2016**, *125*, 1185–1198. [CrossRef]
50. Glotch, T.D.; Kraft, M.D. Thermal Transformations of Akaganéite and Lepidocrocite to Hematite: Assessment of Possible Precursors to Martian Crystalline Hematite. *Phys. Chem. Min.* **2008**, *35*, 569–581. [CrossRef]